

BARYCENTER KINEMATICS IN LOCAL GROUP ANALOGUES

I. A. LÓPEZ-PAREDES 

Escuela de Ingeniería y Ciencias, Tecnológico de Monterrey, Ave. Eugenio Garza Sada 2501, Monterrey 64849, NL, Mexico and
Departamento de Física, Universidad de los Andes, Cra. 1 No. 18A-10 Edificio Ip CP 111711 Bogotá, Colombia

J. E. FORERO-ROMERO 

Departamento de Física, Universidad de los Andes, Cra. 1 No. 18A-10 Edificio Ip CP 111711 Bogotá, Colombia;
je.forero@uniandes.edu.co and
Observatorio Astronómico, Universidad de los Andes, Cra. 1 No. 18A-10 Edificio H CP 111711 Bogotá, Colombia

Version March 12, 2026

ABSTRACT

We present a new way to identify systems similar to our Local Group (LG) of galaxies in cosmological simulations. Our method uses as a new constraint the speed and direction of the LG’s center of mass, which we can measure accurately from cosmic microwave background data. When we apply these criteria to different cosmological simulations and compare the results with traditional selection methods, we find statistically significant differences. Our approach produces simulated galaxy pairs where the relative M31 velocity is less radial (2% to 7% difference over the mean) and more tangential (1% to 3% difference over the mean) than in cases that do not take into account the barycenter speed. The radial change pattern appears consistently across all cosmological models we test, showing that matching the observed barycenter velocity has a measurable effect when modeling and interpreting Local Group-like systems.

Subject headings: Local Group, N-body simulations, barycenter kinematics

1. INTRODUCTION

Understanding the orbit between M31 and the Milky Way (MW) is key to explaining how the Local Group (LG) evolved (Hartl & Strigari 2024). Recent research challenges the old view that this orbit is mostly head-on (radial), suggesting instead that it has more sideways motion than previously thought (van der Marel et al. 2019; Salomon et al. 2021). These studies rely on cosmological simulations to establish expectations for the tangential velocity components. To study LG dynamics, previous work typically identify similar galaxy pairs in simulations by applying specific criteria to halo pairs, including their masses, approach speed, distance, and isolation from other large structures (Forero-Romero et al. 2013; Sawala et al. 2023; Hartl & Strigari 2022).

We identified an important measurement that previous studies haven’t used when defining LG-like systems. This measurement is the LG’s barycenter velocity (\mathbf{v}_b), which we can determine precisely from cosmic microwave background (CMB) data (Planck Collaboration et al. 2020). We use this constraint in two ways. First, we consider its magnitude (v_b). Second, we examine the direction, measured as the angle (θ) between the barycenter velocity vector and the position vector of M31 relative to the MW (\mathbf{r}), as shown in Figure 1. We express this angle more conveniently as $\mu = \cos \theta$, which comes from the dot product of the unit vectors for \mathbf{v}_b and \mathbf{r} .

Previous studies couldn’t use the barycenter velocity because they worked with simulations that were too small in volume. Recently, Forero-Romero & Sierra-

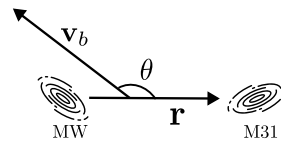


FIG. 1.— Diagram showing the alignment between key quantities used to select LG analogues. \mathbf{v}_b represents the barycenter velocity of the LG and \mathbf{r} shows the position of M31 relative to the MW.

Porta (2022) showed that peculiar velocities can be inaccurate in small simulation boxes due to power spectrum limitations. Using simulations with volumes ranging from 100 to 2967 Mpc across, they demonstrated that accurate kinematic properties require boxes at least 1 Gpc across. Both theoretical arguments and simulation results support this conclusion.

In this paper, we use simulations to measure how including the barycenter velocity constraint affects the predicted radial and tangential velocities of M31 relative to the MW. We also explore how these effects vary across simulations with different cosmological parameters.

Our paper is organized as follows: Section 2 covers the observational constraints, Section 3 describes the simulations used and the different cosmological models. In Section 4, we explain how we select LG analogues using both *traditional* criteria and our new approach. Section 5 presents and discusses our findings, and Section 6 summarizes our conclusions.

2. OBSERVATIONAL CONSTRAINTS

TABLE 1

SUMMARY OF OBSERVED REFERENCE VALUES. THE COLUMNS REPRESENT, RESPECTIVELY: THE PHYSICAL OBSERVABLE, ITS MEASURED VALUE, THE CORRESPONDING UNITS, AND THE BIBLIOGRAPHIC SOURCE.

Observable	Value	Units	Source
v_b	620 ± 15	km s^{-1}	Planck Collaboration et al. (2020)
$(l, b)_{v_b}$	$(271.9 \pm 2.0, 29.6 \pm 1.4)$	deg	Planck Collaboration et al. (2020)
r_{MW}	8.29 ± 0.16	kpc	McMillan (2011)
$(l, b)_{\text{MW}}$	$(359.944215 \pm 0.000006, -0.046079 \pm 0.000009)$	deg.	Yusef-Zadeh et al. (1999)
r_{M31}	761 ± 11	kpc	Li et al. (2021)
$(l, b)_{\text{M31}}$	$(121.174409 \pm 0.000022, -21.572996 \pm 0.000022)$	deg.	Evans et al. (2010)
$v_{r, \text{M31}}$	-109.3 ± 4.4	kms^{-1}	van der Marel et al. (2012)
$v_{t, \text{M31}}$	82.4 ± 31.2	kms^{-1}	Salomon et al. (2021)
μ	-0.88 ± 0.01	adim.	This work

Table 1 summarizes the key observational values used to calculate μ . We obtain the barycenter velocity of the LG from cosmic microwave background (CMB) measurements (Planck Collaboration et al. 2020). The positions of both M31 and the MW are well known from previous studies. For the Sun-to-Galactic Center distance, we use the value from McMillan (2011), who derived this by fitting MW mass models to observational data. The Galactic Center position comes from VLA measurements reported by Yusef-Zadeh et al. (1999). For M31, we use the distance measured by Li et al. (2021) using Cepheid variable stars, and coordinates from the Chandra Source Catalog (Evans et al. 2010).

To calculate the relative position vector from M31 to MW (\mathbf{r}) and determine μ , we use a Monte Carlo approach. We build a covariance matrix using coordinate measurement error ellipses (from NASA/IPAC Extragalactic Database) and sample from a multivariate normal distribution. The uncertainties in Table 1 represent the standard deviations of these samples. Our method yields an M31-MW separation of 765 ± 11 kpc, matching observations reported by Chamberlain et al. (2022). To compute μ , we generate normal distribution samples for \mathbf{v}_b and the distances to MW and M31. We then compute the dot product between \mathbf{v}_b and \mathbf{r} , finding $\mu = -0.88 \pm 0.01$. This result shows a strong anti-alignment between these vectors.

3. SIMULATION

For this study, we use the AbacusSummit simulation suite (Maksimova et al. 2021; Garrison et al. 2021). We analyze the base simulation box with 6912^3 particles in a $2 \text{ Gpc}/h$ volume. Because the simulation snapshot is at redshift $z = 0.1$, we use the halos' peculiar velocities to project their positions to present-day values.

We begin with the primary cosmology (c000), which uses the Planck2018 Λ CDM model with massive neutrinos. We then analyzed 91 additional cosmologies. These include: c009 (without neutrino mass), c019 and c020 (with varied neutrino species counts), and four secondary cosmologies (c001-c004) that test different scenarios such as low Ω_c , wCDM (c002), high N_{eff} , and low σ_8 .

We also study ten reference cosmologies (c010, c012-c018, c021-022) that match models from other major projects, mostly using massless neutrinos. For wider parameter testing, we include simulations with a linear derivative grid (c100-c116) with small changes across eight parameters, and an unstructured emulator grid (c130-c181) covering broader parameter ranges. All cosmologies use the same τ value (0.0544) and most included

60 meV neutrinos, consistent with Planck 2018 results.

4. SELECTION OF LG ANALOGUES

We use halos identified with the CompaSO Halo Finder (Hadzhiyska et al. 2021), with selection criteria similar to those in Forero-Romero & Sierra-Porta (2022). First, we selected halos with maximum circular velocities $V_{\text{max}} > 200 \text{ km s}^{-1}$. From these, we identify isolated pairs as two halos, A and B, that are each other's nearest neighbors. We also require that no third halo with a maximum circular velocity greater than halo B's can be found within three times the pair's separation distance. We define halo A as the one with the greater maximum circular velocity, which we designated as M31. This forms our main sample, typically containing about 8×10^5 pairs per simulation box.

From this main sample, we create two sub samples:

The first subsample, which we call *traditional*, includes pairs meeting these conditions:

- Total pair mass between $[0.5, 5.0] \times 10^{12} M_{\odot}$
- Separation between halos less than $1 \text{ Mpc } h^{-1}$
- Negative radial relative velocity of M31 with respect to the MW ($v_r < 0 \text{ km s}^{-1}$), after accounting for cosmic expansion

The second subsample, which we call *realistic*, includes all the *traditional* criteria plus these additional barycenter velocity conditions:

- Barycenter speed greater than the observed value, including the uncertainty ($v_b > 605 \text{ km s}^{-1}$)
- Alignment value less than the observed value, including the uncertainty ($\mu < -0.87$)

We use inequalities rather than narrow ranges around the observed values because this approach: (1) captures the observed trends that the barycenter speed is unusually high and the alignment shows strong anti-alignment, and (2) allows us to keep more pairs in our sample that satisfy these conditions.

Nonetheless, we include for completeness a variation of the *realistic* subsample, hereafter referred to as *centered*, which replaces the one-sided bounds with a symmetric interval around the observed mean values:

- $500 \text{ kms}^{-1} < v_b < 740 \text{ kms}^{-1}$
- $-0.80 < \mu < -0.96$

The *traditional* subsample typically contains about 2×10^5 pairs per simulation box, while the *realistic* and *centered* sample contain about 10^4 pairs.

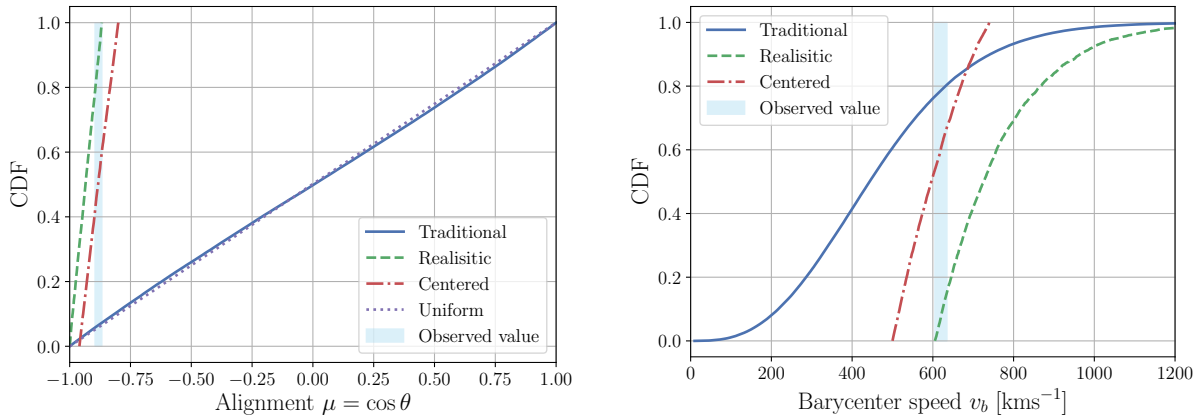


FIG. 2.— Left panel: cumulative distribution of μ , the cosine of the angle between the barycenter velocity of the LG and the position vector of M31 relative to the MW. We also plot a uniform distribution from -1 to 1 for comparison. Right panel: Cumulative distribution for the barycenter speed v_b of the Local Group.

4.1. Statistical Tests

Using the simulations, we compute the cumulative probability distributions for μ and three key Local Group properties:

- Total Local Group mass (M_{LG})
- Radial velocity of M31 relative to the MW (v_r)
- Tangential velocity of M31 relative to the MW (v_t)

To measure how our barycenter velocity constraints affect these properties, we compare the mean values between the *traditional* and *realistic* pair distributions. We also use two-sample Kolmogorov–Smirnov (KS) tests to determine if these differences are statistically significant, with p -values below 0.05 considered significant.

5. RESULTS

5.1. Base cosmology

Figure 2 shows the cumulative distributions of μ and v_b in the base cosmology (c000). These distributions illustrate the key features of our barycenter velocity constraints used to select LG analogues. The μ distribution reveals that \mathbf{v}_b and \mathbf{r} in simulated *traditional* LG pairs tend to be either aligned or anti-aligned. We confirm this by comparing against a uniform distribution using a KS test, which shows statistically significant differences ($p < 0.05$). Using the same statistical method, we also find that the distribution is not symmetric with a slight tendency towards alignment.

We find statistically significant differences between *traditional* and *realistic* pairs in M31’s radial velocity distribution. For radial velocity (v_r), the mean value increases by 5%, indicating a smaller radial speed. The differences in M31’s tangential velocity distribution and total mass (M_{LG}) are not statistically significant.

Figure 3 shows the mean v_r as a function of v_b and μ for the *traditional* pairs in the base cosmology. The figure indicates that smaller radial velocities correspond to higher values of v_b and more extreme values of μ i.e. more aligned or anti-aligned pairs. In contrast, no clear relationship is observed for the tangential velocity.

5.2. All cosmologies

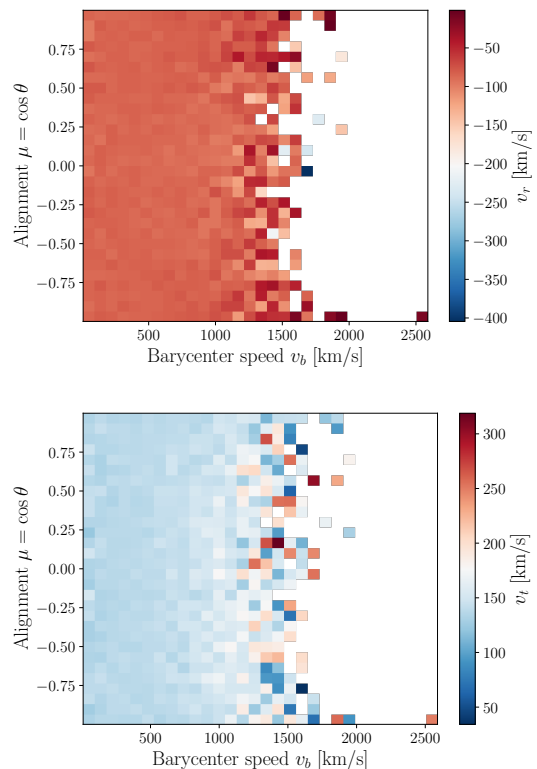


FIG. 3.— Mean velocity components of M31 relative to the MW as a function of v_b and μ in the base cosmology (c000) for the *traditional* sample. The top panel shows v_r and the bottom panel shows v_t .

Our barycenter velocity constraints consistently affect the distributions of both v_r and v_t compared to *traditional* constraints across different cosmological models.

Figure 4 shows how the mean values of tangential and radial velocities change across all cosmologies. *Realistic* pairs consistently show less negative v_r , with mean differences between -2% to -7%. On the other hand, v_t tends to increase for *realistic* pairs. The effect in this case is weaker, with changes between -1% and 3%.

This stronger effect in v_r is also reflected in the significance tests. Figure 5 shows the p -values of the KS tests

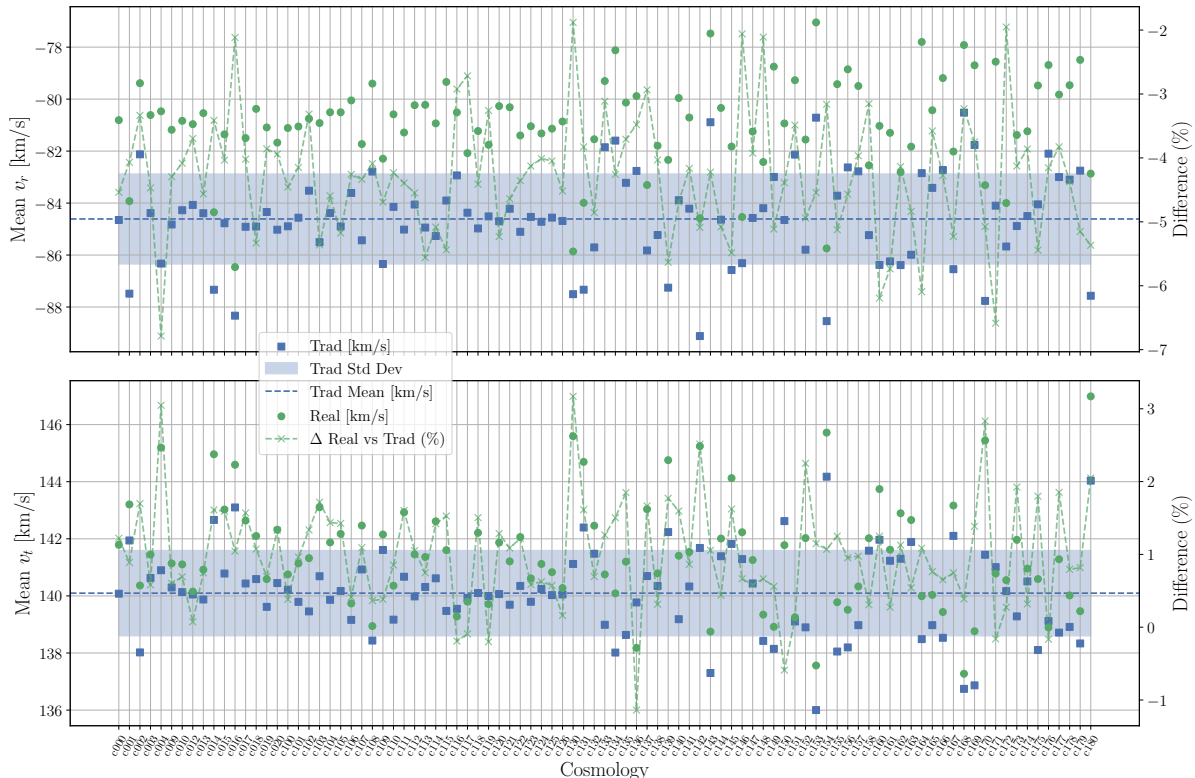


FIG. 4.— Mean values of M31 velocity distributions in all cosmologies (top panel shows v_r and the bottom panel v_t). The main y-axis corresponds to the mean values of the velocities for *traditional* and *realistic* pairs. The secondary y-axis shows the percentage difference in mean values of *realistic* pair distributions compared to the mean of *traditional* pair distributions in each cosmology. Dashed lines and shaded regions represent the average and standard deviation of the mean values of *traditional* pair distributions for all cosmologies

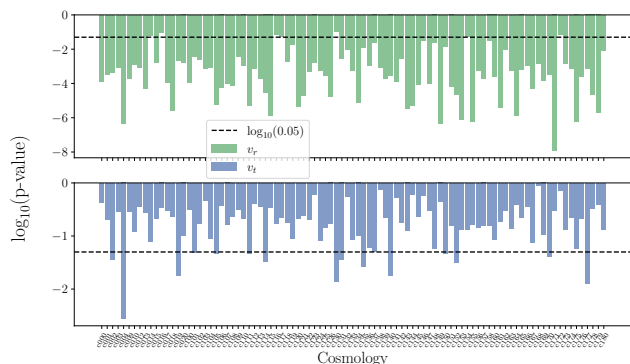


FIG. 5.— Statistical significance of the differences between *realistic* and *traditional* selection criteria for radial velocity v_r (top panel) and tangential velocity v_t (bottom panel). The p -values shown are from two-sample Kolmogorov-Smirnov tests across all cosmologies.

between *traditional* and *realistic* pairs velocity distributions. Among the 93 cosmologies we study, the differences in radial velocity distribution are significant in 86 models, while tangential velocity distribution show significant differences in 15 cosmologies. The effect on total mass (M_{LG}) is significant in only 9 cosmologies. Table 2 summarizes for each cosmology, which combinations of observables display statistically significant differences between *traditional* and *realistic* or *centered* pairs.

We calculated the average shift in the observables across cosmologies with significant differences, and to

TABLE 2
NUMBER OF COSMOLOGIES WHERE THE DIFFERENCE BETWEEN TRADITIONAL AND REALISTIC OR CENTERED PAIRS WAS STATISTICALLY SIGNIFICANT FOR EACH COMBINATION OF OBSERVABLES.

Observable	N. cosmo. (Realistic)	N. cosmo. (Centered)
None	6	47
v_r only	65	34
v_t only	1	9
v_r and v_t	12	3
M_{LG} only	0	0
v_r and M_{LG}	7	0
v_t and M_{LG}	0	0
All three	2	0
Total	93	93

avoid selection bias, we repeated the procedure across all cosmologies. The results shown in table 3 further show the mentioned trend in the measured shift of the observables. The change in v_r seen in the *realistic* sample is the largest and most robust across cosmologies. The mean change of roughly 4.6% in the significant subset remains almost the same (4.5%) when averaged over all cosmologies. The *centered* sample follows the same trend but with smaller magnitudes. Tangential velocity behaves differently. The mean difference in significant cosmologies is small (around 1.6% for the *realistic* sample), and when averaged over all cosmologies the value drops below 1%. For the *centered* sample the average change is negative (which correspond smaller velocities), but the magnitude is below 1% for the both averages (across sig-

TABLE 3
 PERCENTAGE DIFFERENCES IN THE DISTRIBUTIONS OF THE M31 VELOCITY COMPONENTS (v_r AND v_t) AND THE TOTAL MASS OF THE LOCAL GROUP (M_{LG}). FOR EACH OBSERVABLE AND SAMPLE TYPE, THE TABLE REPORTS THE MEAN DIFFERENCE RELATIVE TO THE TRADITIONAL SAMPLE, COMPUTED (I) USING ONLY THE COSMOLOGIES WHERE THE DIFFERENCE IS STATISTICALLY SIGNIFICANT AND (II) USING ALL 93 COSMOLOGIES. THE LAST COLUMN GIVES THE NUMBER OF COSMOLOGIES WHERE THE KS TEST INDICATES A SIGNIFICANT DIFFERENCE BETWEEN THE DISTRIBUTIONS.

Observable	Sample	Mean difference I (%)	Mean difference II (%)	Significant cosmologies (out of 93)
v_r	Realistic	-4.64	-4.51	86
	Centered	-2.83	-2.14	37
v_t	Realistic	1.63	0.96	15
	Centered	-0.75	-0.33	12
M_{LG}	Realistic	-0.83	-0.31	9
	Centered	-	-0.06	0

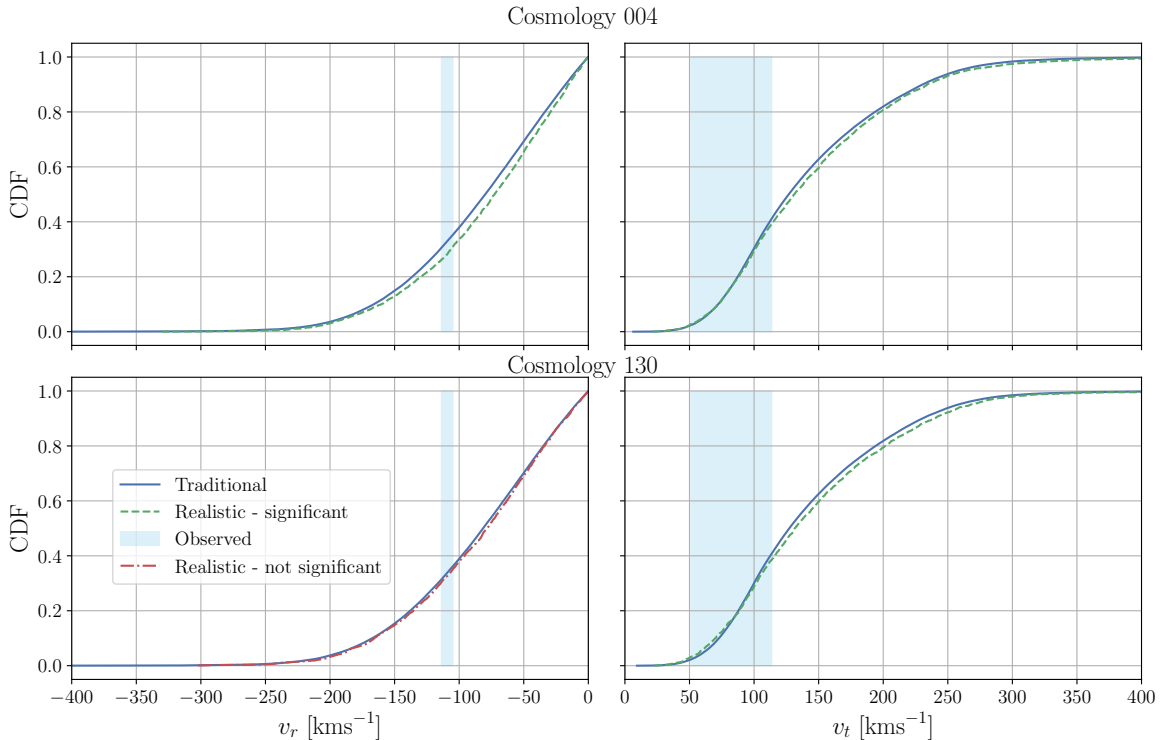


FIG. 6.— Cumulative distributions of M31 velocities relative to the MW in cosmology 004 and cosmology 130, where we found the biggest difference in the mean between *traditional* and *realistic* pairs. In cosmology c004, the difference in both v_r (-7%) and v_t (3%) was statistically significant. In cosmology 130 only the difference in v_t (3%) was statistically significant.

nificant cosmologies and across all cosmologies). M_{LG} has the weakest effect, with changes below 1 percent and significant differences in only 9 cosmologies for the *realistic* sample and none for the *centered*.

The cosmologies in which we found the biggest differences in v_r and v_t between *traditional* and *realistic* pairs were c004 (a baseline Λ CDM with low $\sigma_8 = 0.75$) and c130 (an emulator grid around baseline cosmology). In cosmology c004, the difference is statistically significant for both observables, with mean differences of 7% in v_r and 3% in v_t . In cosmology 130, the difference is significant only in v_t , with a mean difference of 3%). The corresponding cumulative distributions are shown in Figure 6.

Although the barycenter-based selection produces mean shifts that are statistically significant given the large sample sizes, the absolute shifts (\sim a few km s^{-1}) are small compared to the typical velocity dispersion of

LG analogues (tens of km s^{-1}); thus the effect is a modest kinematic refinement rather than a major physical change.

5.3. Cosmological parameters

To explore which cosmological parameters most strongly influence whether the differences in v_r and v_t between *traditional* and *realistic* pairs are statistically significant, we trained a Random Forest classifier using the KS-test outcome (significant vs. not significant) as the target. However, the *realistic* filter introduces a class imbalance. For v_r , in 86 out of 93 cosmologies we found significant differences and for v_t , only in 11. Under these conditions, the classifier is dominated by the majority class and cannot reliably learn the minority class. This is reflected on the performance metrics obtained: 0.48 macro F1 score and weighted F1 score of 0.89.

For this reason we also considered the *centered* filter

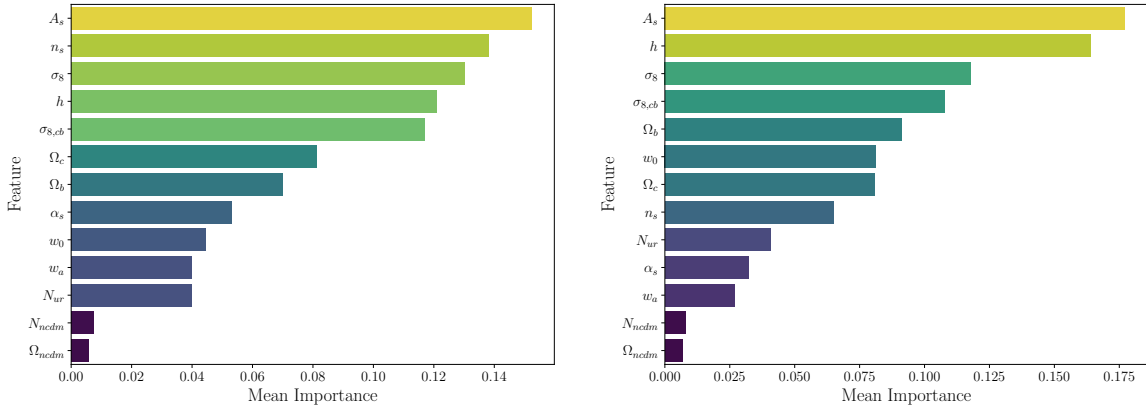


FIG. 7.— Relative importance of various cosmological parameters for predicting whether the difference in M31’s velocities between *centered* and *traditional* pairs is statistically significant. The left panel shows the parameter importance for v_r , and the right panel for v_t . Importance is calculated using a Random Forest algorithm.

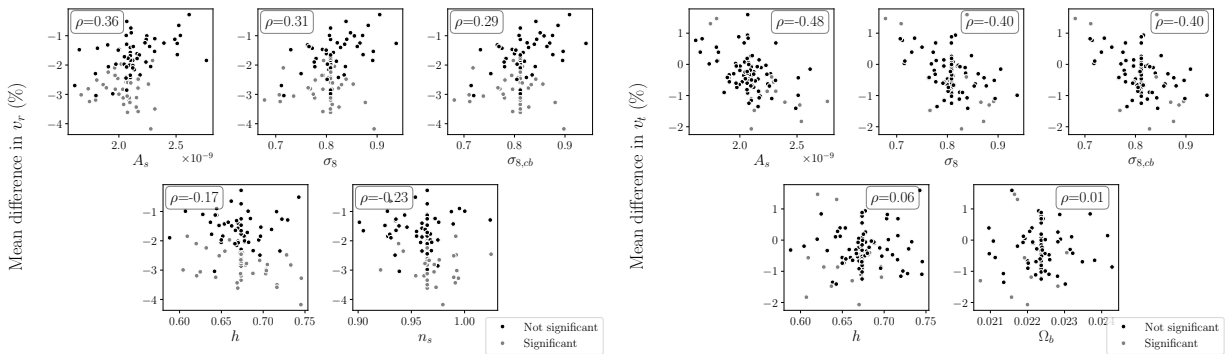


FIG. 8.— Scatter plots of the mean difference in M31’s velocities between *centered* and *traditional* pairs versus the most important cosmological parameters for predicting whether a cosmology leads to significant differences. The left panel corresponds to v_r , and the right panel for v_t . For each parameter, ρ is the calculated Pearson correlation coefficient with respect to the mean difference in the velocity.

which defines a broader range around the mean observed values of v_b and μ . This filter produces a more balanced distribution of significant and non-significant cosmologies. In this case the F1 macro score was 0.55 and the weighted F1 score was 0.58. For this sample, the mean importance obtained for each parameter with a stratified K-fold validation is shown in figure 7. The most important parameter for determining significance for both velocity components was A_s (scalar perturbation amplitude).

We then computed Pearson correlation coefficients between the mean velocity differences and individual cosmological parameters. Under the *realistic* filter, v_r shows no measurable correlation, while v_t shows a moderate negative correlation ($\rho \approx -0.45$) with both A_s and σ_8 . Under the *centered* filter however, the mean difference in v_r exhibits moderate positive correlations ($\rho \approx 0.3$), with both A_s and σ_8 , while the correlation with v_t remains unchanged.

The appearance of A_s and σ_8 among the most influential parameters in the Random Forest Analysis, and their moderate correlations under the *centered* filter, suggests that the amplitude of matter fluctuations may play a role in setting how strongly barycenter kinematics affect Local Group analogue velocities. A higher fluctuation amplitude deepens gravitational potentials and may influence how coherent the barycenter motion is relative to halo orbits. Exploring these mechanisms, however,

requires a dedicated physical study and lies beyond the scope of this work. The results presented here should therefore be regarded as exploratory, illustrating statistical trends rather than establishing physical causation.

6. CONCLUSION

In this work, we explored the barycenter velocity (\mathbf{v}_b) as a new kinematic constraint for defining Local Group (LG) analogues. This quantity has very low observational uncertainty but was not included in previous studies due to the need for sufficiently large simulation volumes to achieve numerical convergence in peculiar velocities (Forero-Romero & Sierra-Porta 2022). Using simulations from the AbacusSummit project, with a box size of $2 \text{ Gpc } h^{-1}$, we have shown that including this constraint introduces a small but systematic shift in the predicted velocity distributions of M31. We demonstrated this effect by comparing LG analogues selected using our proposed constraints (*realistic* pairs) with those selected using *traditional* constraints (separation distance less than $1 \text{ Mpc } h^{-1}$ and negative radial velocity). Our results show that in the *realistic* pairs, M31 tends to have a smaller radial velocity v_r and larger tangential velocity v_t compared to the *traditional* pairs. We quantified this effect using the difference in means and assessed its significance through two-sample Kolmogorov-Smirnov tests.

This effect is consistent across cosmological models and is particularly robust for v_r . In our analysis of 93 differ-

ent cosmologies, we found significant differences in the radial velocity distribution for 86 models, while the tangential velocity distribution showed significant differences in 15 cosmologies. The mean differences between *realistic* and *traditional* pairs were -4.5% for v_r (less radial) and 1% for v_t (more tangential), averaged across all cosmologies.

We also found that A_s and σ_8 are the cosmological parameter that most strongly influences the significance of differences in radial and tangential velocity distributions. However, further work is needed to understand the influence of cosmological parameters on LG kinematics. Similarly, while we have demonstrated statistical differences in velocity distributions, a deeper exploration of the physical mechanisms explaining why barycenter kinematics correlate with orbital properties remains for future work. Assessing if these results change our understanding of the Local Group properties and history –for

instance in light of studies such as Chamberlain et al. (2022), Hartl & Strigari (2024), Benisty & Mota (2025) – is also left for future work.

In summary, our results show that the kinematic constraints proposed in this work consistently influence the radial and tangential velocities of M31, with effects that are robust across cosmological models. Although small in magnitude, these systematic effects highlight that the LG’s bulk motion encodes useful information about its internal dynamics. Incorporating these new kinematic constraints should therefore be considered when defining LG analogues in future studies.

ACKNOWLEDGMENTS

This work made use of the NASA/IPAC Extragalactic Database (NED), funded by the National Aeronautics and Space Administration and operated by the California Institute of Technology.

REFERENCES

- Benisty, D., & Mota, D. 2025, *Astronomy & Astrophysics*, 698, A43, doi: 10.1051/0004-6361/202553846
- Chamberlain, K., Price-Whelan, A. M., Besla, G., et al. 2022, *The Astrophysical Journal*, 942, 18, doi: 10.3847/1538-4357/aca01f
- Evans, I. N., Primini, F. A., Glotfelty, K. J., et al. 2010, *The Astrophysical Journal Supplement Series*, 189, 37, doi: 10.1088/0067-0049/189/1/37
- Forero-Romero, J. E., Hoffman, Y., Bustamante, S., Gottlöber, S., & Yepes, G. 2013, *The Astrophysical Journal*, 767, L5, doi: 10.1088/2041-8205/767/1/L5
- Forero-Romero, J. E., & Sierra-Porta, D. 2022, *The Astrophysical Journal*, 939, 16, doi: 10.3847/1538-4357/ac92ea
- Garrison, L. H., Eisenstein, D. J., Ferrer, D., Maksimova, N. A., & Pinto, P. A. 2021, *Monthly Notices of the Royal Astronomical Society*, 508, 575, doi: 10.1093/mnras/stab2482
- Hadzhiyska, B., Eisenstein, D., Bose, S., Garrison, L. H., & Maksimova, N. 2021, *Monthly Notices of the Royal Astronomical Society*, doi: 10.1093/mnras/stab2980
- Hartl, O. V., & Strigari, L. E. 2022, *Monthly Notices of the Royal Astronomical Society*, 511, 6193, doi: 10.1093/mnras/stac413
- . 2024, *The Milky Way and M31 Orbital History: Did the Local Group evolve in isolation?*, arXiv, doi: 10.48550/arXiv.2411.07370
- Li, S., Riess, A. G., Busch, M. P., et al. 2021, *The Astrophysical Journal*, 920, 84, doi: 10.3847/1538-4357/ac1597
- Maksimova, N. A., Garrison, L. H., Eisenstein, D. J., et al. 2021, *Monthly Notices of the Royal Astronomical Society*, 508, 4017, doi: 10.1093/mnras/stab2484
- McMillan, P. J. 2011, *Monthly Notices of the Royal Astronomical Society*, 414, 2446, doi: 10.1111/j.1365-2966.2011.18564.x
- Planck Collaboration, Aghanim, N., Akrami, Y., et al. 2020, *Astronomy & Astrophysics*, 641, A6, doi: 10.1051/0004-6361/201833910
- Salomon, J.-B., Ibata, R., Reylé, C., et al. 2021, *Monthly Notices of the Royal Astronomical Society*, 507, 2592, doi: 10.1093/mnras/stab2253
- Sawala, T., Teeriaho, M., & Johansson, P. H. 2023, *Monthly Notices of the Royal Astronomical Society*, 521, 4863, doi: 10.1093/mnras/stad883
- van der Marel, R. P., Fardal, M., Besla, G., et al. 2012, *The Astrophysical Journal*, 753, 8, doi: 10.1088/0004-637X/753/1/8
- van der Marel, R. P. v. d., Fardal, M. A., Sohn, S. T., et al. 2019, *The Astrophysical Journal*, 872, 24, doi: 10.3847/1538-4357/ab001b
- Yusef-Zadeh, F., Choate, D., & Cotton, W. 1999, *The Astrophysical Journal*, 518, L33, doi: 10.1086/312058

This paper was built using the Open Journal of Astrophysics L^AT_EX template. The OJA is a journal which

provides fast and easy peer review for new papers in the **astro-ph** section of the arXiv, making the reviewing process simpler for authors and referees alike. Learn more at <http://astro.theoj.org>.